JOURNAL OF Applied Polymer SCIENCE

Fundamental Thermo-Mechanical Property Modeling of Triglyceride-Based Thermosetting Resins

John La Scala,[1,2] Richard P. Wool[2]

[1]Department of the Army, Army Research Laboratory, RDRL-WMM-C, Aberdeen Proving Ground, Maryland 21005

[2]Department of Chemical Engineering, University of Delaware, Newark, Delaware 19716

Correspondence to: J. La Scala (E-mail: john.j.lascala.civ@mail.mil.)

ABSTRACT: The glass transition temperature (T_g) of acrylated triglycerides was clearly a function of the level of acrylation of triglyceride-based polymers and was modeled using simple empirical relationships. We began by calculating the distribution of unsaturation sites in plant oils. We assumed a binomial distribution of chemical functionality that was added to these unsaturation sites to calculate the distribution of epoxides, acrylates, and reacted acrylates to predict the crosslink density, thermal softening, and dynamic mechanical behavior. The glass transition temperatures of n-acrylated triglycerides were used as the relaxation temperatures of acrylated oils with a broad distribution of functionality for prediction of the modulus as a function of temperature. Essentially, the percent drop in the elastic modulus is equal to the percentage of n-acrylated triglycerides in the acrylated oil with T_g less than that of the ambient temperature. The tan (δ) was also accurately predicted based on the percentage change of n-functional triglycerides as the temperature changes from one relaxation temperature to the next. © 2012 Wiley Periodicals, Inc. J. Appl. Polym. Sci. 000: 000–000, 2012

KEYWORDS: crosslinking; glass transition; thermosets; renewable resources; relaxation

Received 5 October 2011; accepted 16 April 2012; published online
DOI: 10.1002/app.37927

INTRODUCTION

Triglycerides, the main component of plant oils, have been used to produce thermosetting resins for composites applications.[1] These resins have similar properties and performance[2] relative to unsaturated polyester (UPE) resins.[3] Triglyceride monomers act as crosslinkers, while low molecular weight reactive diluents, such as styrene, are added to modify the properties of the polymer and lower the resin viscosity. The low viscosities of these resins make them ideal for inexpensive polymer composite fabrication processes, such as vacuum assisted resin transfer molding. The high strength and modulus of these resins makes them suitable as a matrix for supporting reinforcement fibers, such as glass, flax, or jute.[2,4]

Triglyceride-based resins are an attractive alternative to petroleum-based resins because they are inexpensive, have desirable properties, and are derived from renewable resources. Triglycerides (Figure 1) are composed of three fatty acids connected by a glycerol center. There are numerous ways of chemically converting triglycerides to useful monomers for composites applications.[1,2] Using the unsaturation sites on fatty acids is the most common way for making triglyceride crosslinking agents for thermosetting resins.[2]

Structure–property modeling for thermosetting resins seeks to predict polymer properties based on the molecular structure of the resin components. Plant oils typically contain 5–10 distinct fatty acids.[5,6] For plant oils with 10 different fatty acids, there are 900 possible distinct triglyceride molecules, making plant oils a highly complex mixture of molecules. Functionalizing triglycerides (i.e., chemically modifying their unsaturation sites) to form monomers only increases the number of distinct molecules in the resin mixture. Pure plant oils are currently used as the starting product for plant-oil-based thermosetting resins because bio-refining of triglycerides is still in its infancy. The triglycerides in the plant oils are not fractioned off or further refined to generate highly pure triglycerides for each degree of unsaturation and chain length. This is in stark contrast to petroleum derived resins that use highly refined petroleum distillates as components to form the monomers. Therefore, structure–property modeling of triglyceride-based resins seems to be a very difficult task. Yet, previous work has shown that the glass transition temperature (T_g), room temperature tensile modulus, and room temperature tensile strength can be predicted based on the known distribution of triglycerides in the starting plant oil.[7] However, because of the large distribution of molecules in plant oils, the glass transition is often very broad.[2] For

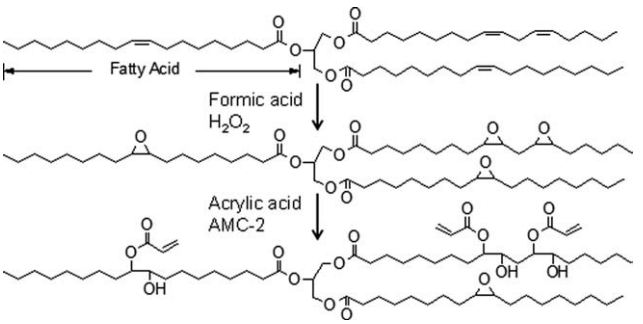

Figure 1. The epoxidation (1st reaction) and acrylation (2nd reaction) of triglycerides.

structural and mechanical purposes, the modulus reduction with temperature is often more important than the particular T_g. As of yet, the breadth of the glass transition has not been predicted for plant oil-based polymers.

Percolation theories, including the "Twinkling Fractal Theory (TFT) of the Glass Transition"[8] can be used to help determine to breadth of the glass transition. These theories are based on the hard-to-soft matter transition, which is essentially the glass transition: the glass transition is arrived at by heating a hard cold glassy material to a suitable temperature whereby the material softens.[8,9] As T_g is approached from above, dynamic solid fractal clusters begin to form and eventually percolate rigidity at T_g.[8] This leads to a continuous solid (glassy) fraction, P_G, near T_g. Using TFT, P_G is [Eq. (1)]:

$$P_G \sim 1 - [(1 - p_c)T/T_g] \quad (1)$$

where $p_c \approx 1/2$ is the rigidity percolation threshold.[8] Other percolation theories predict a similar relation to determine the glassy fraction. To determine the exact relationship between glassy fraction and temperature, the TFT uses a factor called the vibrational density of states that is a function of frequency and is material specific.[8] Other percolation theories either ignore this term or use fitting parameters to enable fit of the theory to a particular polymer system.[9,10] It appears possible to measure the vibrational density of states for a material, but doing so is difficult.[8] In all, accurate prediction of the glassy fraction as a function of temperature *a priori* is either difficult or not currently possible.

This work derives a relatively simple method based on polymer composition to extend twinkling fractal theory and percolation theory of the glass transition to enable accurate prediction of the glass transition. Previous work shows how the glass transition temperature of plant oil-based polymers can be predicted based on the level of chemical functionality (i.e., average number of chemical functional groups added to triglyceride unsaturation sites) and also shows that the distribution of functionality can be predicted.[7] This work shows that the triglyceride functionality distribution can be used to determine the rubbery fraction of a polymer relative to the glassy fraction. Using this, the TFT and percolation predications of the glass transition can be used to develop a model to predict the modulus and general dynamic mechanical properties of triglyceride-based polymers as a function of temperature as well as the breadth of the glass transition, while also providing verification to the Twinkling Fractal Theory and percolation theories of the glass transition.

EXPERIMENTAL SECTION

Monomer Synthesis

The plant oils used in this work have similar molecular weights, but different levels of unsaturation, *U*, ranging from 2.8-6.4 sites per triglyceride (Table I).[5] Olive oil, cottonseed oil, canola oil, corn oil, soybean oil, and linseed oil were purchased from Sigma-Aldrich. A model triglyceride, triolein (99%, Sigma-Aldrich) was also used. DuPont Corporation (Wilmington, DE) provided the genetically engineered high oleic soybean oil (HOSO). These plant oils and model triglyceride have considerably different fatty acid distributions, but have similar molecular weights.[5]

Epoxidized samples (Figure 1) were made by reacting the unsaturated sites of oils and model triglyceride with a mixture of formic acid and hydrogen peroxide as presented elsewhere.[7,11] The extent of epoxidation was measured using ^{1}H-NMR[7,12] with a Bruker AC250 Spectrometer (Billerica, MA) of 250.13 MHz using a spectral window of ± 2000 Hz, 0.427 Hz/pt digital resolution, 16 scans at 293 K, and 90° pulse width. Table I lists the extent of epoxidation and level of epoxidation, *E*, for all the oils used in this work, which was 96% on average.

Acrylate monomers were prepared by reacting the epoxide groups of epoxidized oils and epoxidized model triglyceride with acrylic acid as presented elsewhere[7,11] (Figure 1) using AMC-2 (Aerojet Chemicals) as a catalyst.[13] Each oil was maximally acrylated by adding 1.1 moles of acrylic acid per epoxide group to the reaction mixture. Oils were acrylated to different extents (~ 20%-~ 94%) to see the effect of acrylation level (i.e., the number of acrylates per triglyceride) on a given plant oil.[7] We selected the desired extent of acrylation, and added 1.1 times the required amount of acrylic acid to the reaction mixture. The acrylated triglycerides were purified using an ether extraction.[7,11] The extents of acrylation and level of acrylation, *A*, were measured using ^{1}H-NMR[7,12] as per the epoxidized oils. Using both methods, the level of functionalization was varied from 0.65 to 5.8 acrylates per triglyceride (Table I). The extent of acrylation was 94% on average for the maximally acrylated oils.

Polymer Preparation

Two types of polymers were prepared from the acrylated triglycerides: homopolymerized acrylated triglycerides and copolymers with 85 mol % styrene (i.e., 85 mol % styrene to 15 mol % acrylated triglycerides). A constant weight percentage of styrene (33 wt %) was also used. A constant mol % styrene as the acrylation level is changed allows the formation of a polymer network that varies only as a result of difference in the level of acrylation. Using a constant weight percent styrene does not guarantee this, but generally does allow for a simpler analysis of the glass transition temperature. However, T_g did not follow the Fox equation[14] or a simple model when using constant weight percent styrene, while it did follow a simple relationship when using constant styrene molar concentration. As a result, this work analyzes the results of constant molar styrene concentration rather than constant weight percent styrene. Yet, constant weight percent styrene produces very similar results and

Table I. The Level of Triglyceride Functionality and Molecular Weight

Oil	Oil molecular weight (g/mol)	Unsaturation sites per triglyceride	Extent of epoxidation	Epoxides per triglyceride	Extent of acrylation (based on epoxides)	Acrylates per triglyceride (acrylation level)	Mol. Wt. of acrylated triglycerides (g/mol)
Olive Oil	874 ± 20	2.8 ± 0.1	0.92 ± 0.04	2.6 ± 0.2	0.92 ± 0.04	2.5 ± 0.1	1096 ± 30
HOSO[a]	875 ± 15	3.0 ± 0.1	0.93 ± 0.04	2.8 ± 0.2	0.94 ± 0.04	2.7 ± 0.1	1114 ± 25
HOSO	875 ± 15	3.0 ± 0.1	0.93 ± 0.04	2.8 ± 0.2	0.79 ± 0.05	2.2 ± 0.1	1078 ± 25
HOSO	875 ± 15	3.0 ± 0.1	0.93 ± 0.04	2.8 ± 0.2	0.61 ± 0.06	1.7 ± 0.05	1042 ± 20
HOSO	875 ± 15	3.0 ± 0.1	0.93 ± 0.04	2.8 ± 0.2	0.39 ± 0.05	1.1 ± 0.05	999 ± 20
HOSO	875 ± 15	3.0 ± 0.1	0.93 ± 0.04	2.8 ± 0.2	0.23 ± 0.08	0.65 ± 0.05	967 ± 20
Triolein	885 ± 3	3.0 ± 0.1	0.93 ± 0.04	2.8 ± 0.2	0.97 ± 0.04	2.8 ± 0.1	1131 ± 10
Cottonseed oil	860 ± 20	3.8 ± 0.1	0.95 ± 0.03	3.5 ± 0.2	0.93 ± 0.04	3.3 ± 0.1	1154 ± 30
Canola oil	880 ± 20	3.9 ± 0.1	0.97 ± 0.03	3.8 ± 0.2	0.94 ± 0.03	3.5 ± 0.1	1193 ± 30
Corn oil	872 ± 20	4.4 ± 0.1	0.98 ± 0.02	4.3 ± 0.2	0.96 ± 0.03	4.0 ± 0.1	1229 ± 30
Soybean oil	873 ± 15	4.6 ± 0.1	0.97 ± 0.02	4.4 ± 0.2	0.95 ± 0.02	4.2 ± 0.1	1246 ± 25
Soybean oil	873 ± 15	4.6 ± 0.1	0.97 ± 0.02	4.4 ± 0.2	0.64 ± 0.04	2.8 ± 0.1	1145 ± 25
Soybean oil	873 ± 15	4.6 ± 0.1	0.97 ± 0.02	4.4 ± 0.2	0.57 ± 0.04	2.5 ± 0.1	1123± 25
Soybean oil	873 ± 15	4.6 ± 0.1	0.97 ± 0.02	4.4 ± 0.2	0.43 ± 0.05	1.9 ± 0.1	1080± 25
Soybean oil	873 ± 15	4.6 ± 0.1	0.97 ± 0.02	4.4 ± 0.2	0.25 ± 0.05	1.1 ± 0.05	1023 ± 20
Linseed oil	873 ± 15	6.4 ± 0.1	0.95 ± 0.02	6.1 ± 0.2	0.98 ± 0.02	5.8 ± 0.1	1388 ± 25
Linseed oil	873 ± 15	6.4 ± 0.1	0.95 ± 0.02	6.1 ± 0.2	0.85 ± 0.02	5.2 ± 0.1	1345 ± 25
Linseed oil	873 ± 15	6.4 ± 0.1	0.95 ± 0.02	6.1 ± 0.2	0.67 ± 0.03	4.1 ± 0.1	1266 ± 25
Linseed oil	873 ± 15	6.4 ± 0.1	0.95 ± 0.02	6.1 ± 0.2	0.57 ± 0.04	3.5 ± 0.1	1223 ± 25
Linseed oil	873 ± 15	6.4 ± 0.1	0.95 ± 0.02	6.1 ± 0.2	0.48 ± 0.02	2.9 ± 0.1	1179 ± 25
Linseed oil	873 ± 15	6.4 ± 0.1	0.95 ± 0.02	6.1 ± 0.2	0.36 ± 0.05	2.2 ± 0.1	1129 ± 25
Linseed oil	873 ± 15	6.4 ± 0.1	0.95 ± 0.02	6.1 ± 0.2	0.21 ± 0.05	1.3 ± 0.05	1064 ± 20

[a]HOSO, a genetically engineered High Oleic Soybean Oil.

conclusions. The styrene (99%) was purchased from Aldrich Chemicals, Milwaukee, WI.

A concentration of 0.015 g/mL Hi Point 90 (Witco, Marshall, TX) was used as the free-radical initiator for all samples. Hi Point 90 is composed of a mixture of methyl ethyl ketone peroxides with relatively low molecular weights and different decomposition temperatures. To reduce oxygen free-radical inhibition, the resin was purged with nitrogen gas before curing. The resin was then poured into vertical molds. The vertical molds consisted of a silicone rubber mold (Dow Corning, Midland, MI) sandwiched between two aluminum plates using binder clamps. The silicone molds had four equally spaced slots 11 mm wide, 5 mm thick, and 83 mm tall for Dynamic Mechanical Analysis (DMA) samples. A sheet of Kapton film was used on both sides of the silicone rubber to help make a very flat surface. All mold components were sprayed with PTFE Release Agent Dry Lubricant (Miller-Stephenson, Danbury, CT) to ease demolding.

The samples were cured in an Isotemp Oven (Fisher Scientific). The temperature was ramped from 30 to 90°C at a rate of 5°C/min and the samples were cured at 90°C for 2 h. The temperature was then ramped to 120°C at 5°C/min. The samples were post-cured for 2 h at this temperature. The samples for DMA were polished down to approximate dimensions of 55 mm long × 9 mm wide × 3.5 mm thick using 320 grit sandpaper on a polishing wheel.

Fourier Transform Infrared Spectroscopy

In-situ FTIR was used to calculate the overall extent of cure of the resins after postcure as described elsewhere.[15] A Nicolet Magna 860 FTIR operating in transmission mode with 4 cm^{-1} resolution was used. A drop of the resin was sandwiched between two 25 mm diameter NaCl disks (International Crystal Labs) separated by a 0.025 mm thick Teflon™ spacer (International Crystal Labs) and placed in a cell holder that was heated to the set point and controlled within ± 0.1°C. All resin mixtures were cured at 90°C for 2 h and post-cured at 120°C for an additional 2 h. FTIR spectra, comprised of 16 scans, were taken every 2 min during the cure reaction. These results can be used also to determine cure kinetics, but are not considered in this analysis.

Thermo-Mechanical Testing

The thermo-mechanical properties of the triglyceride-based polymers were tested using a Rheometrics Solids Analyzer II (Rheometrics Scientific). Before testing, the exact sample dimensions were measured. The samples were tested in three-point bend geometry. The temperature was ramped from −60°C to 180°C at a rate of 2°C/min, with a frequency of 1 Hz, and a strain of 0.01%. The temperature was controlled with

Table II. The Ultimate Conversion of Triglyceride Homopolymers and Copolymers with Styrene

Oil	Acrylates per triglyceride	Homopolymer acrylate conversion	Copolymers	
			Acrylate conversion	Styrene conversion
Olive oil	2.5 ± 0.1	0.96 ± 0.02	1.0 ± 0	0.91 ± 0.02
HOSO	2.7 ± 0.1	0.96 ± 0.02	1.0 ± 0	0.91 ± 0.02
HOSO	2.2 ± 0.1	0.97 ± 0.02	1.0 ± 0	0.91 ± 0.02
HOSO	1.7 ± 0.05	0.98 ± 0.02	1.0 ± 0	0.90 ± 0.02
HOSO	1.1 ± 0.05	0.98 ± 0.02	1.0 ± 0	0.89 ± 0.02
HOSO	0.65 ± 0.05	0.98 ± 0.02	1.0 ± 0	0.85 ± 0.02
Triolein	2.8 ± 0.1	0.96 ± 0.02	1.0 ± 0	0.92 ± 0.02
Cottonseed oil	3.3 ± 0.1	0.95 ± 0.02	0.99 ± 0.01	0.92 ± 0.02
Canola oil	3.5 ± 0.1	0.95 ± 0.02	0.99 ± 0.01	0.93 ± 0.02
Corn oil	4.0 ± 0.1	0.95 ± 0.02	0.99 ± 0.01	0.94 ± 0.02
Soybean oil	4.2 ± 0.1	0.95 ± 0.02	0.99 ± 0.01	0.93 ± 0.02
Soybean oil	2.8 ± 0.1	0.96 ± 0.02	1.0 ± 0.01	0.92 ± 0.02
Soybean oil	2.5 ± 0.1	0.97 ± 0.02	1.0 ± 0.01	0.91 ± 0.02
Soybean oil	1.9 ± 0.1	0.97 ± 0.02	1.0 ± 0.01	0.90 ± 0.02
Soybean oil	1.1 ± 0.05	0.98 ± 0.02	1.0 ± 0.01	0.89 ± 0.02
Linseed oil	5.8 ± 0.1	0.94 ± 0.02	0.98 ± 0.01	0.95 ± 0.02
Linseed oil	5.2 ± 0.1	0.94 ± 0.02	0.98 ± 0.01	0.95 ± 0.02
Linseed oil	4.1 ± 0.1	0.95 ± 0.02	0.99 ± 0.01	0.94 ± 0.02
Linseed oil	3.5 ± 0.1	0.95 ± 0.02	0.99 ± 0.01	0.93 ± 0.02
Linseed oil	2.9 ± 0.1	0.96 ± 0.02	1.0 ± 0.01	0.92 ± 0.02
Linseed oil	2.2 ± 0.1	0.97 ± 0.02	1.0 ± 0.01	0.91 ± 0.02
Linseed oil	1.3 ± 0.05	0.98 ± 0.02	1.0 ± 0.01	0.90 ± 0.02

a Rheometrics Environmental Controller, and liquid nitrogen was used for cooling below room temperature. This experiment was repeated at least three times for each sample.

RESULTS

Extent of Cure

The styrene and acrylate conversions were measured as a function of time t, by relating the absorbance (ABS) of the peak of interest to the peak heights of internal standards as measured by FTIR. The ultimate conversion, x_u, was calculated using the following equation[15]:

$$x_u = 1 - \left(\frac{ABS(final)_{\text{peak}}}{ABS(t=0)_{\text{peak}}}\right)\left(\frac{ABS(t=0)_{\text{standard}}}{ABS(final)_{\text{standard}}}\right) \quad (2)$$

The peak at 990 cm^{-1} represents a vibrational mode of the vinyl group on acrylate groups.[16,17] The peak at 910 cm^{-1} represents both the acrylate[16,17] and styrene carbon–carbon double bond.[15] The internal standards used were the peaks at 1744 cm^{-1}, corresponding to the ester groups on the triglycerides,[16] and the peak at 700 cm^{-1}, representing the aromatic C—H stretch on styrene.[15] Neither of these groups was affected by the polymerization reaction.

The ultimate conversion of styrene was greater than 0.90 and the ultimate conversion of acrylate groups was over 0.94 for all samples (Table II). The ultimate conversion of acrylate groups decreased slightly as the initial number of acrylates per triglyceride increased for samples without styrene comonomer. This occurred because there is an increased likelihood for unreacted acrylates to be attached to crosslinked triglycerides and become trapped in highly crosslinked regions as the level of acrylation increased. When styrene comonomer was used, the level of acrylation had minimal effect on the acrylate conversion. The presence of styrene was expected to increase the conversion of acrylate groups because styrene increases the conversion at which gelation occurs and reduces diffusion limitations.[18,19] The conversion of styrene did not change as the comonomer content was increased, but it did increase slightly as the level of acrylate functionality increased.

Dynamic Mechanical Analysis

Dynamic mechanical analysis gives a number of measures of the glass transition temperature. The inflection point of the storage modulus (E') as a function temperature is the midpoint between the glassy and rubbery regions, and as such, is a measure of T_g. The temperature at which the peak in the loss modulus (E'') occurs is often used, and generally, but not always, corresponds to the inflection point in the modulus curve. The tan (δ) is the ratio of the loss modulus to the storage modulus. The temperature at which the tan (δ) maximum occurs is also a measure of the glass transition temperature, but is generally 10°C or more higher than the loss modulus peak or storage modulus inflection point.[20]

The DMA behavior of these polymers was fairly similar to that of other thermosetting polymers[21] (Figure 2). In the glassy region, the resins had a high modulus (~ 1−3 GPa). After the glass transition, all of the resins exhibited a plateau rubbery modulus that was relatively insensitive to temperature. Acrylated triglyceride/styrene copolymers had higher glass transition temperatures relative to acrylated triglyceride homopolymers (no styrene) because styrene's rigid aromatic planar ring structure interferes more with chain mobility compared to that of an acrylate. Homopolymerized triglyceride resins exhibited a broad glass transition/relaxation compared to commercial vinyl esters or unsaturated polyesters.[21,22] The breadth of the glass transition increased as the level of acrylation per triglyceride increased[7] as has been seen for other polymer systems as crosslinking is increased.[20,21] The breadth of the glass transition was reduced for styrene-copolymers relative to acrylated triglyceride homopolymers. As a result, the difference in temperatures between the loss modulus peak and tan (δ) peak for homopolymers was greater than that for copolymers. There is no evidence of phase separation in these resins, as all resins had a single, albeit broad, glass transition. Also, all of the samples were clear indicating neither macro- nor micro-phase separation occurred. For all samples, the loss modulus maximum peak appeared at temperatures slightly lower than the storage modulus inflection point, while the tan (δ) peak occurred at slightly higher than the storage modulus inflection point.

The rubbery modulus was calculated from values of the DMA storage modulus that were within the plateau region of the modulus. The exact point selected was at the temperature where the modulus did not change with further increases in temperature. For samples without styrene, the rubbery modulus reached a plateau at 50–100°C above the maximum in tan (δ). Comonomer content had a large effect on this temperature relative to the tan (δ) maximum. For samples with 85 mol % comonomer, the temperature at which the rubbery modulus reached a plateau occurred at 30–50°C above the maximum in tan (δ). The experimental crosslink density values were calculated from the rubbery moduli of the polymers. Rubber Elasticity Theory[23] shows that the molecular weight between crosslinks, M_c, and crosslink density are related to the modulus of elasticity, E, of rubbers[7,20,24] [Eq. (3)]:

$$E = 3RT\rho/M_c = 3RTv \quad (3)$$

where R is the ideal gas constant, T is the absolute temperature, v is the crosslink density, and ρ is the polymer density. The polymer densities increased slightly with the acrylation level and ranged from 1.04 to 1.11 g/cm^3. Styrene content had little effect on the density. The temperature corresponding to the maximum in the loss modulus was taken as T_g of the polymer.[20]

The crosslink density increased for plant oil-based polymers with and without styrene as a function of the acrylation level.[7] The crosslink density increased linearly with the level of acrylation for homopolymerized triglycerides.[7] Similarly, the crosslink density increased linearly with the level of acrylation for triglyceride copolymers with styrene, but only at 2.5 or higher acrylates per triglyceride.[7] The nonlinear increase in the crosslink density occurred because at low levels of acrylate functionality, the functional groups mainly linearly extended the polymer chains rather than crosslinking them. However, at higher levels of acrylate functionality, each additional functional group increased the crosslink density. This was not observed in the homopolymerized triglycerides because of their higher crosslink density. Also as expected, the crosslink density was higher for homopolymers of triglycerides relative to that of copolymers of triglycerides and styrene.[7] Again, this is expected because styrene is a reactive diluent that decreases the crosslink density.

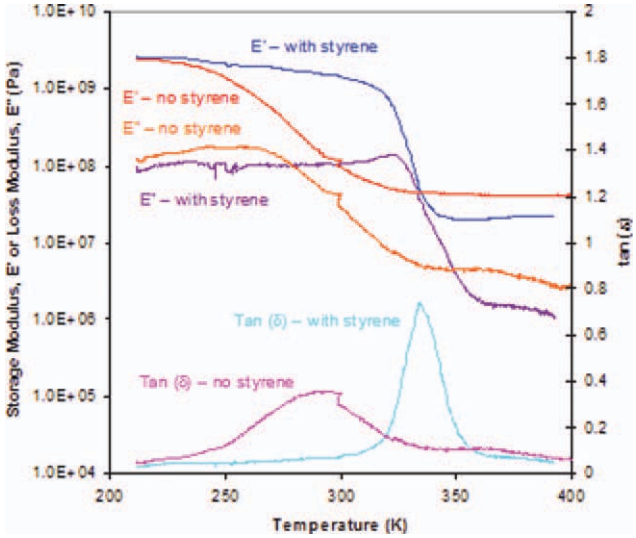

Figure 2. The dynamic mechanical properties of maximally acrylated canola oil homopolymerized (no styrene) and copolymerized with styrene. [Color figure can be viewed in the online issue, which is available at wileyonlinelibrary.com.]

The glass transition temperature increased linearly as a function of acrylation level for samples with 85 mol % styrene and without styrene (Figure 3). The glass transition temperature according to the loss modulus [Eq. (4)] was linearly approximated as a function of the number of acrylates per triglyceride, A, for homopolymerized triglycerides:

$$T_g = 14.8 \times A + 205.3 \quad [\mathrm{K}] \quad (4)$$

For acrylated triglycerides copolymerized with 85 mol % styrene, the T_g according to the loss modulus [Eq. (5)] is:

$$T_g = 27.3 \times A + 213 \quad [\mathrm{K}] \quad (5)$$

T_g of these polymers ranged from below room temperature to well over room temperature. This makes sense as the samples were rubbery at low levels of acrylation and rigid at high acrylation levels. T_g was not dependent on the oil type, in that different oils acrylated to the same level had similar T_g. Furthermore, T_g of maximally acrylated oils and partially acrylated oils with the same level of functionalization were similar. The T_g for a given acrylated oil with 85 mol % styrene was higher than that of the corresponding homopolymerized sample because the

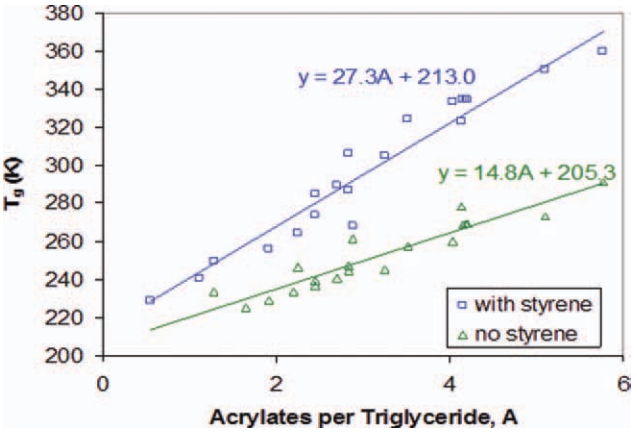

Figure 3. The glass transition temperature as measured by the loss modulus of homopolymerized acrylated oils and acrylated oils copolymerized with styrene. [Color figure can be viewed in the online issue, which is available at wileyonlinelibrary.com.]

aromatic nature of styrene imparts rigidity to the network. These results are in agreement with previous results, which showed that T_g is a simple function of acrylation level (A).[7]

The glass transition temperature according to the tan (δ) is the temperature corresponding to the tan (δ) peak maximum and was similarly found to be linearly proportional to the level of acrylation of the triglycerides. This temperature for acrylated triglyceride homopolymers is [Eq. (6)]:

$$T_g(\tan_{\max}(\delta)) = 28.5 \times A + 197.6 \quad [\mathrm{K}] \tag{6}$$

and for copolymers with styrene is [Eq. (7)]:

$$T_g(\tan_{\max}(\delta)) = 22.4 \times A + 256.3 \quad [\mathrm{K}] \tag{7}$$

For homopolymerized triglycerides, the tan (δ) and loss modulus maxima diverged as the level of acrylation increased. In addition for homopolymerized triglycerides, the T_g according to tan (δ) was a stronger function of the acrylation level than T_g according to the E'', while the opposite trend occurred for triglycerides copolymerized with styrene. The difference can be seen in the DMA plots for each of these polymers (Figure 2). The details of this will be explained and proven later in this work, but essentially the following is theorized. The viscous fraction (or rubbery fraction) increased slowly as a function of temperature in the glassy region for samples with styrene because only low functional triglycerides became rubbery in the general glassy regime, while the styrene fraction and highly functionalized triglycerides remained glassy. This narrowed the T_g breadth relative to homopolymerized samples and caused the loss modulus peak to remain relatively consistent with the E' inflection point. Thus, most of the sample's relaxation occurred upon the temperature at which the highly functional triglycerides/styrene clusters relax. This occurred at or after the major softening point of the material, causing the temperature of $\tan_{\max}$ (δ) to rise with acrylation level. For homopolymerized triglycerides, as low functional triglycerides reached their glass transition temperature, they became rubbery. Because there is no styrene to help rigidize the system, an earlier onset to the loss modulus peak occurred as acrylation level increased.

Triglyceride Distribution Calculation

The distribution of polymerized acrylate groups on triglycerides is necessary to determine the breadth of the glass transition for acrylated triglycerides. Thus, this section first examines the distribution of unsaturation functionality on triglycerides and then how that distribution can be used to calculate the polymerized acrylate functionality and properties.

Unmodified Triglycerides Unsaturation Distribution

The percentage of fatty acids in a given oil is well known and is relatively easy to determine experimentally and theoretically for a given oil.[5,6] The distribution of unsaturated triglycerides in a given oil is needed to predict various properties, especially the dynamic mechanical spectrum and the T_g breadth of the polymer. Yet, the distribution of unsaturated triglycerides is not well known because the fatty acids are not randomly distributed on triglycerides.[25] Triglycerides are assembled in nature by attaching successive fatty acids on glycerol,[25] regardless of whether the assembly occurs through the glycerol phosphate pathway, the dihydroxyacteone pathway, or the monoglyceride pathway. Enzymes interact with both the fatty acid(s) already assembled onto the glyceride as well as the fatty acid to be attached to the glycerol center.[25]

Analysis of plant oils has revealed a number of regular patterns in the distribution of fatty acids between the sn-1, sn-2, and sn-3 positions on the glycerol (i.e., the 1st, 2nd (middle), and 3rd fatty acid on the triglyceride).[6] Saturated fatty acids and those with chain lengths greater than 18 carbon atoms are almost exclusively found at the equivalent sn-1 and sn-3 positions [Eq. (8)].[6] The 1,3-Random, 2-Random Hypothesis was proposed by Vander Wal[26] and Coleman and Fulton.[27] This hypothesis assumes that two different pools of fatty acids are separately and randomly distributed to the 1,3- and 2-positions of the glycerol molecules. Thus, the sn-1 and sn-3 positions should have equivalent fatty acid distributions. The amount of each triglyceride composed of fatty acid A, B, and C can be calculated using [Eq. (8)]:

$$\%\text{sn-ABC} = [\text{mol \% A at 1, 3-pos.}][\text{mol \% B at 2-pos.}][\text{mol \% C at 1, 3-pos.}] \times 10^{-4} \tag{8}$$

However, to do this calculation, separation of the fatty acids into two different pools must be done.

The Evan's Hypothesis proposed rules to estimate the positional distribution of fatty acids in plant oils.[28] Saturated acids and those with chain lengths greater than 18 carbon atoms are first distributed equally at the 1- and 3-positions. Oleic and linolenic acids are then distributed randomly on the unfilled 1-, 2-, and 3-positions. When the 1- and 3-positions are filled, the excess is added to the 2-position. All remaining positions are filled by linoleic acid. Previous researchers have shown that the Evans Hypothesis and 1,3-Random, 2-Random Hypothesis accurately predict the unsaturation distribution for soybean oil and for most plant oils[6,12] and in particular the fatty acid distributions for all of the plant oils used in this work can be used to accurately calculate the triglyceride distribution.

Table III. The Distribution of Unsaturation Sites, P(U), and the Unsaturation Level, U, for the Various Oils Used in this Work

		Mole percent triglycerides with 0-9 unsaturation sites, P(u)									
Oil	U	0	1	2	3	4	5	6	7	8	9
Olive	2.82	0.1	4.6	39.7	14.4	2.5	0.3	0.0	0.0	0.0	0.0
HOSO	2.97	0.0	1.9	21.0	59.2	6.4	7.8	0.4	0.3	0.0	0.0
Cotton	3.77	0.3	3.1	16.3	18.7	31.9	15.0	13.1	0.2	0.0	0.0
Canola	3.91	0.0	0.6	8.5	33.2	27.3	19.4	7.6	2.6	0.5	0.1
Corn	4.33	0.0	1.3	6.5	16.4	28.3	27.2	18.6	0.9	0.0	0.0
Soybean	4.60	0.0	1.0	5.9	13.9	24.9	25.4	20.1	6.9	1.0	0.0
Linseed	6.59	0.0	0.2	0.8	2.4	5.7	9.4	18.0	19.4	17.2	26.2

The distribution of unsaturation sites (Table III) was determined from the calculated fatty acid distribution.[5,12] The level of unsaturation of a given triglyceride was simply the sum of the unsaturation sites on the constituent fatty acids. The percentage of all triglycerides with a given functionality, $P(U)$, is just the summation of the percentage of all triglycerides with U unsaturation sites per triglyceride on average [Eq. (9)]:

$$P(U) = \sum_{u=i+j+k} \%\mathrm{sn} - \mathrm{A(i)}B\mathrm{(j)C(k)} \tag{9}$$

where i, j, and k are the number of unsaturation sites on fatty acids A, B, and C. It is apparent that the distribution of unsaturation sites is very different for the different oils, even for oils that have similar unsaturation levels. In most cases, the distribution of unsaturation sites extended from 0 to 9 sites per triglyceride. In some of these cases, such as soybean oil, the distribution is normal. However, for linseed oil, the distribution is bimodal. Some oils, such as cottonseed oil, only have triglycerides with 0-6 unsaturation sites because of the lack of linolenic acid in these oils. As a result, their triglyceride distribution was skewed. Fortunately, only a very small percentage of triglycerides had no functionality. These triglycerides would act as plasticizer in crosslinked polymer, lowering the T_g and modulus. However, in some oils, such as olive oil, a significant fraction of the triglycerides have only 1 unsaturation site. Monounsaturated triglycerides can only act as linear chain extenders, and thus will decrease the crosslink density of the polymer. Furthermore, most of the oils contained a very large fraction of di-unsaturated oils. At most 2 fatty acids of the di-unsaturated triglycerides can be attached into the polymer network. The third arm will act as a plasticizer and reduce the polymer properties.

Chemically Modified Triglycerides

How functionality is distributed during chemical reaction as a function of extent of reaction is unknown. However, NMR analysis of epoxidation indicates that the process is mostly random and unlikely to be highly selective at high extents of reaction. Epoxide peaks of typical fatty acids have four basic peak assignments: monoepoxidized fatty acid with no remaining unsaturation sites (2.90 ppm), epoxide protons on the δ-9 and δ-10 positions, the δ-12 and δ-13 positions, or the δ-15 and δ-16 positions on mono-epoxidized fatty acids with at least 1 unsaturation site (2.93 ppm), the protons attached to the δ-9 and δ-13 carbon atoms of di-epoxy fatty acids and the δ-9 and δ-16 carbon atoms of tri-epoxy fatty acids (2.92–3.03 ppm), and the hydrogen atoms attached to the δ-10 and δ-12 carbon atoms of di-epoxy fatty acids (3.03–3.18 ppm).[11,12] In particular, NMR results showed that highly monounsaturated oils did not develop peaks at 2.98 ppm and 3.10 ppm until very high extents of reaction. Highly unsaturated oils first produce peaks at 2.93 ppm, which then shrank as the peaks at 2.98 ppm and 3.10 began to grow. As a result, for this work, the distribution of epoxide functionality will be assumed random. We cannot do such a measurement for acrylated and polymerized triglycerides. Therefore, these distributions will also be assumed to be random.

The equations for calculating the distribution of functional groups can be generalized for any series of reactions. Using the distribution of reactive sites before reaction, $F(N)$, the distribution of functional groups after reaction can be determined using a binomial distribution.[29] The probability of having n functional groups on a triglyceride with N reactive sites was calculated using Eq. (10):[29]

$$P(N, n, \xi) = C(N, n)\xi^n(1-\xi)^{N-n}F(N) \tag{10}$$

where ξ is the extent of reaction and $C(N,n)$ is the number of different ways the n functional groups can be arranged on the triglyceride with N reactive sites (i.e., $C(N,n)$ is the combinatorial function or binomial coefficient). These probabilities were calculated for all 55 possible triglycerides combinations (i.e., the number of possible combinations of having n functional groups on a triglyceride with N reactive sites). The percentage of n-functional triglycerides, $p(n,\xi)$, is:

$$p(n, \xi) = \sum_N P(N, n, \xi) \tag{11}$$

This method assumes that the addition of functional groups to triglycerides was completely random. However, previous results showed that functional groups have a slight preference for the fatty acid to which they attach.[11,12] On the other hand, the relative preferences of functional groups for different fatty acids were of the same order of magnitude. Furthermore, the studies that found preferential attachment of functional groups only examined the initial rates of the reaction. The effect of pre-existing functional groups on a fatty acid on the addition of another functional group has not been studied. These studies

Applied Polymer SCIENCE

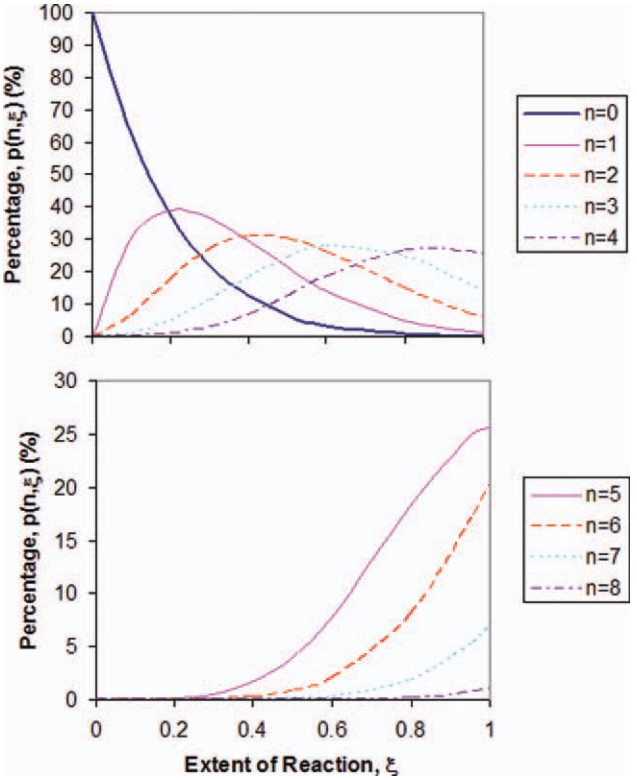

Figure 4. The distribution of n-functional triglycerides as a function of extent of functionalization in soybean oil. The conversion of triglycerides with 9 added functional groups was omitted from the plot because its percentage was approximately 0 at all extents of reaction. Note the two different scales on the y-axes of the plots. [Color figure can be viewed in the online issue, which is available at wileyonlinelibrary.com.]

also indicated that the effects of preferential addition should be dampened at high conversions.[11,30] Last, in this work, we are only concerned with the level of functionality of a given triglyceride. The location of the functional groups on the fatty acid and the acid to which they are attached is not important. Therefore, the distributions of functional groups should be fairly accurate; however, they are only approximate. Furthermore, the exact percentage of triglycerides with a certain number of functional groups is not as important as the general trends observed.

The percentage of triglycerides with n-unreacted sites was calculated as a function of the extent of reaction, ξ, and is shown for functionalized soybean oil in Figure 4. At $\xi = 0$, none of the triglycerides had any added functional groups. At $\xi = 1$, the functional distribution was equal to the original unsaturation distribution. Over the course of the reaction, the percentage of triglycerides with 0 functional groups initially decreased fairly steeply, then leveled out and approached 0% nearly asymptotically. Triglycerides with fewer functionality than the average level of unsaturation of the oil increased to a maximum and then decreased to the initial percentage of triglycerides with the same number of unsaturation sites as functional groups. In addition, these maxima occurred at lower extents of reaction as the level of unsaturation of the oil increased. Triglycerides with more functional groups than the average oil unsaturation reached a maximum at $\xi = 1$. In all cases, triglycerides with fewer functional groups reached a maximum percentage at extents of reaction less than 1.

This model was tested by epoxidizing 33 and 67% of the unsaturation sites on triolein. The triglyceride distribution model predicted that the solids should be 74% of the total mass and the liquids should be 26% of the mass. Di- and tri-epoxy triglycerides with a single epoxy per fatty acid were solid at room temperature. Mono-epoxy and unepoxidized triolein were liquids at room temperature. As a result, the solid and liquid products were separated by filtration.

The functionalities of both samples were analyzed using ^{1}H-NMR. The level of epoxidation of the solid fraction, F_S, and liquid fraction, F_L, were found to be 2.35 and 0.84, respectively, for the 67% epoxidized sample. The corresponding percentage of mono-epoxy triglycerides, P_1, in the liquid fraction was [Eq. (12)]:

$$P_1 = 100F_L \tag{12}$$

and the difference from 100% yielded the percent of unepoxidized triglycerides. The percentage of di-epoxy triglycerides, P_2, in the solid was [Eq. (13)]:

$$P_2 = 300 - 100F_S \tag{13}$$

and the difference from 100 was the percentage of di-epoxy triglycerides. The agreement between experiment and theory was good for the 67% epoxidized sample (Table IV) and the 33% epoxidized sample. Furthermore, the experiment verified the production of a very high relative concentration of mono-epoxy and di-epoxy triglycerides at 33 and 67%, respectively. Error between theory and experiment was a result of error in the predicted triglyceride distributions and the inability to perfectly separate the solid and liquid fractions.

Given an extent of epoxidation and the unsaturation distribution, the distribution of epoxidized triglycerides in a given oil was calculated. Using that distribution, which is slightly different from the unsaturation distribution because of a lack of complete conversion and the extent of acrylation, the acrylate distribution was similarly calculated (Table V). Lastly, the distribution of polymerized acrylate groups in the polymers was calculated (Table V) based on the extent of polymerization (Table II) and the calculated acrylate distribution (Table V). As a result of incomplete reaction, the amount of polymerized acrylates is likely to be significantly lower than the amount of unsaturated triglycerides and the amount of unpolymerized triglycerides is likely to be higher than the original amount of saturated

Table IV. The Theoretical and Experimental Fractions of Epoxidized Triglycerides in the Solid and Liquid Portions of 67% Epoxidized Triolein

Epoxides per triglyceride	Predicted		Experiment	
	Liquid	Solid	Liquid	Solid
0	14	0	16	0
1	86	0	84	0
2	0	60	0	63
3	0	40	0	37

Table V. The Distribution of Functionality in Soybean Oil

Functional groups per triglyceride	Unsaturation, U (mol %)	Acrylate functionality, Y_n (mol %)	Effectively reacted acrylates, X_n (mol %)
0	0.0	0.2	1.6
1	1.0	2.3	9.0
2	5.9	9.2	20.9
3	13.9	19.1	27.6
4	24.9	26.9	23.3
5	25.4	23.6	12.6
6	20.1	14.2	4.2
7	6.9	4.0	0.7
8	1.0	0.5	0.0
9	0.0	0.0	0.0
Average	4.60	4.21	3.21

triglycerides. This will reduce various properties of the polymerized oils, including the crosslink density and glass transition temperature of the resulting polymers.

Property Modeling

Various structure–property relationships need to be determined to predict dynamic mechanical properties of these thermosetting polymeric resins. First, crosslink density must be determined to calculate the rubbery modulus. Glass transition modeling must be done then to relate the functional triglyceride distribution to the dynamic mechanical properties as a function of temperature.

Crosslink Density Modeling

The crosslink density is affected by the functionality of the crosslinker molecule. Vinyl polymers are typically represented as having two functional groups, *f*, per vinyl group, *n*.[31] The number of functional groups on a crosslinker that polymerizes and leads to another crosslinked molecule is *m*, where $m \leq f$. For example, triglycerides with $m = 1$ functional group are dangling chain-ends. The functionality, *m*, and the number of crosslinked chains, N_{xc}, per triglyceride are related [Eq. (14)]:

$$N_{xc} = 3m/2 - 3 = 3n - 3 \tag{14}$$

Therefore, with *m* in the range 0-18, the number of crosslink chains varies from 0-24 per triglyceride, depending on the functionality. The positional distribution of the functional groups does not affect N_x. Therefore, the structure of the triglyceride (i.e., three chemically linked fatty acids) has no effect on the crosslink density except that it allows each triglyceride molecule to have a different number of functional groups and crosslinks.

The crosslink chains and junctures are shown in Figure 5 for triglycerides with 3 and 6 polymerized functional groups. Each polymer chain stemming from a polymerized acrylate is composed of styrene or acrylated units, but always links to another triglyceride with 2 or more polymerized acrylate groups (otherwise this would be a dangling chain end). The number of crosslinks chains are 1.5 and 6 for triglycerides with 3 and 6 polymerized functional groups, respectively, and the number of crosslink junctures (N_{xj}) were 1 and 4, respectively. The positional distribution of the functional groups does not affect number of crosslinked chains or crosslink junctures. Therefore, the structure of the triglyceride (i.e. three chemically linked fatty acids) has no effect on the crosslink density except that it allows each triglyceride molecule to have a larger number of functional groups and crosslinks. Note that the dangling chain ends not highlighted in Figure 5 are still used in calculation of the crosslink density, but were not shaded to more simply illustrate the crosslink chains. Thus, this analysis not only holds for multifunctional triglycerides, but also is applicable to any free-radical crosslinking agent, such as vinyl esters and unsaturated polyesters.

Flory and others have used the principles of branching and crosslinking to derive the crosslink density for addition polymers.[30–32] La Scala and Wool generalized this equation for a mixture of crosslinkers with *n* functionality [Eq. (15)]:[7]

$$c = \theta \sum_{n=2}^{n=9} \phi_n (3n - 3) \tag{15}$$

where *c* is the number of crosslink chains per molecule, ϕ_n is the fraction of triglycerides with *n* polymerizable groups, and θ is the extent of polymerization. The molecular weight between crosslinks is simply the average molecular weight of the monomers, M_{av}, divided by the number of crosslinks per molecule [Eq. (16)]:

$$M_c = M_{av}/c \tag{16}$$

The crosslink density resulting from chemical crosslink chains can then be calculated by dividing the polymer density by M_c.

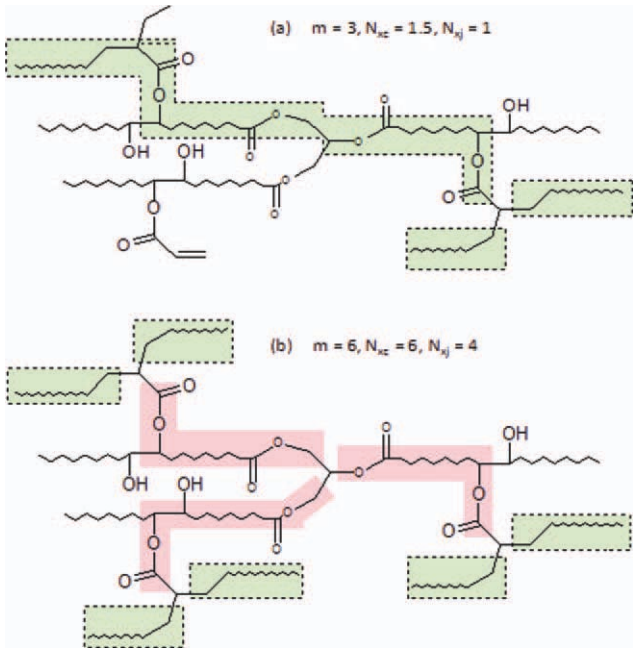

Figure 5. The crosslink chains on triglycerides with (a) m = 3 and (b) m = 6. The outlined green boxes represent ½ crosslinks while the non-outlined pink boxes represent whole crosslinks. The grey circles represent crosslink junctures. [Color figure can be viewed in the online issue, which is available at wileyonlinelibrary.com.]

The La Scala model over-predicted the crosslink density of triglyceride systems as measured from dynamic mechanical analysis because of intramolecular cyclization.[7] Intramolecular cyclization of functional groups on the same triglyceride reduces the number of effective attachment points of this triglyceride to the rest of the network. When a triglyceride reacts with itself before reacting with another triglyceride, it forms a loop that is not attached to the rest of the polymer network. Consequently, this reduces the crosslink density of the resulting polymer. Every time two functional groups react in this way, the effective number of functional groups per triglyceride is reduced by 2. Yet, the model predictions and experimentally determined results were simply shifted from one another by some degree of acrylation. The extent of intramolecular cyclization was quantified by fitting the model results to the experimental results. The shift required to equate the model crosslink density, $\nu_{\text{model}}(\text{A})$, to the experimentally determined crosslink density, $\nu_{\text{exp}}(A)$, was A_{lost} [Eq. (17)][7]:

$$\nu_{\text{model}}(A - A_{\text{lost}}) = \nu_{\text{exp}}(A) \tag{17}$$

Overall, the model predicted that the amount of intramolecular cyclization reduced the effective functionality by approximately 0.7–0.9 acrylates per triglyceride.[7] Therefore, the model accurately predicted the trends in the crosslink density with acrylation level.

Glass Transition Modeling

Relaxation mode modeling of relaxation master curves does not relate to material structure. The relaxation modes are arbitrary frequencies or times along the master curve of the material that illustrate only time-scale dependent softening of the material.[33–35] Time–temperature superposition principle (TTSP) is typically used to reduce the storage and loss modulus data into time–temperature master-curves.[34] The Williams-Landél-Ferry (WLF) equation is used to characterize the temperature dependence of the distribution of relaxation times in viscoelastic materials using three parameters to fit the data, which as of now, cannot be determined from fundamental knowledge of the polymer.[33–37]

Using aspects of the material structure as relaxation modes would be a much better method for understanding and predicting polymer properties and tailoring higher performance materials. The glass transition temperature is clearly a function of the level of acrylation or functionality of triglyceride-based polymers. Furthermore, the glass transitions were narrower for plant oils with narrower fatty acid distributions. Given a perfect chemical network with no dangling chain ends and all chemical functionality effectively reacted, the glass transition should be quite sharp.[35,36,38] An example of this phenomenon is easily visible when examining the glass transition as a function of reactive diluent content. It is well known that the T_g becomes sharper as the reactive diluent content increases partly because the effective extent of cure of the crosslinker increases.[23,39] However, due to distributions of functionality on the crosslinkers, fluctuations in crosslink density across the material, incomplete reaction or ineffective reaction (i.e., intramolecular cyclization), the glass transition broadens.[23,39] Since the distribution of effectively crosslinked triglycerides can be calculated as shown above, it seems reasonable to use the glass transition temperature of 0 through n-functional triglycerides as the relaxation modes for the polymer (Table VI). Although the average triglyceride acrylate functionality can be 3.5, for example, the individual triglycerides only have whole number values of acrylates. Therefore, the relaxation temperatures correspond to the glass transition temperatures of triglycerides with 1, 2, 3,…9 acrylates per triglyceride and are calculated using equations for T_g of homopolymerized oils as a function of acrylation level [eqs. (4) and (6)]. Table VI shows relaxation temperatures based on the loss modulus maximum, T_g [Eq. (4)], and the tan (δ) maximum, $T_g(\tan(\delta))$ [Eq. (6)]. The choice of which relaxation temperature set to use to model the glass transition is explained in the following sections.

Table VI. Relaxation Temperatures for n-Functional Homopolymerized Triglycerides

	Relaxation temperatures (K)	
Level of Functionality	T_g (E'')	T_g (tan (δ))
0	205	198
1	220	226
2	235	255
3	250	283
4	265	312
5	279	340
6	294	369
7	309	397
8	324	426
9	339	454

The Twinkling Fractal Theory and percolation theories of the glass transition state that there the glassy fraction converts to rubbery fractions and the overall glass transition occurs when the rubbery clusters percolate the material. We extended this concept to the modulus of a polymer as a function of temperature to predict the breadth of the glass transition. We postulate that the modulus is proportional to the bond fracture energy or glassy modulus minus the liquid fraction, analogous to the glassy fraction of the material as predicted by percolation theories.[8] In other words, a homopolymerized triglyceride resin that contains 30% di-functional triglycerides and 70% $n > 2$ functional triglycerides should lose $\sim$ 30% of its modulus above the T_g of the difunctional triglycerides ($T_g(n = 2) \sim 233$ K). However, rubbery materials can also support load, so the rubbery modulus, as determined using the predicted crosslink density and Rubber Elasticity Theory,[23] must also be used. Therefore, the modulus of homopolymerized triglycerides at a given relaxation temperature is [Eq. (18)]:

$$E'(T) = E_0^*[1 - P_R(T)/100] + E'(\text{rubbery}) \tag{18}$$

where $P_R(\text{T})$ is the mole percent of rubbery polymer with $T_g(E'')$ less than T [Eq. (19)]:

$$P_R(T) = \sum_{n=0}^{n} X_n \quad \text{for values of } n \text{ where } T_g(n) < T \tag{19}$$

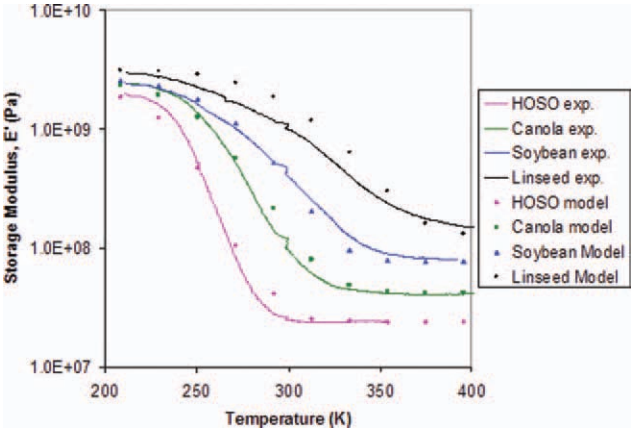

Figure 6. The storage modulus as a function of temperature for selected maximally acrylated and homopolymerized oils as determined by experiment and as modeled. [Color figure can be viewed in the online issue, which is available at wileyonlinelibrary.com.]

where X_n is the mole percent of n-functional triglycerides based on the distribution of effectively crosslinked acrylate groups on the triglycerides in a given oil. The glassy modulus, E_0, was assumed to be 3 GPa at 180 K, a typical number for polymeric materials.[10] E'(rubbery) is calculated based on the crosslink density calculations previously described and using Rubber Elasticity to calculate the rubbery modulus [Eq. (3)]. $T_g(n)$ is the glass transition temperature of n-functional triglycerides. The relaxation modes are thus the glass transition temperature of homopolymerized triglycerides weighted by the percent of each triglyceride with this glass transition temperature. Essentially, as temperature increases, the low functional triglycerides begin to soften allowing a modulus drop, followed by the softening of the mid-functional triglycerides and lastly the high-functional triglycerides. Because triglyceride-based polymers contain a distribution of functionality, the modulus drops significantly as the temperature is increased from very low temperatures (e.g., 200 K) through the T_g of the 9-functional triglycerides (339 K).

Note, Eq. (18) and the analysis below are only valid for crosslinkers that have the same basic structure and type of functionality. In other words, this type of analysis is not valid for mixed crosslinker systems of vinyl esters and unsaturated polyesters, for example. Yet, this type of analysis should be useable for other crosslinker systems, like unsaturated polyesters, but the relaxation temperatures for that system would need to be determined.

The predicted value of the storage modulus using Eq. (18) matched the experimental results well for both maximally acrylated oils (Figure 6) and individual oils acrylated to different extents (Figure 7). The predicted storage modulus was glassy at low temperatures and dropped over the course of the broad glass transition finally reaching a rubbery plateau. There is some deviation between the predicted results and experimental results. These are likely due to slightly incorrect predictions in the triglyceride distribution and the simplifying assumptions in eqs. (18) and (19). In the case of linseed oil, where the model results over predict the modulus, it is likely that there are more low functional triglycerides than predicted. The results show that intramolecular cyclization must be taken into account. Without considering intramolecular cyclization, canola oil would have approximately the same level of effectively polymerized acrylates per triglyceride as soybean oil when accounting for intramolecular cyclization. Yet, the predicted modulus vs. temperature of canola oil does not match the experimental results for soybean oil (Figure 6). Clearly, if intramolecular cyclization was not accounted for in X_n, the model would over predict the results considerably.

The storage modulus can also be predicted for triglycerides copolymerized with styrene using the same relationship of storage modulus as a function of temperature [Eq. (20)] as before [Eq. (18)] with a slightly different function for the mole percentage of rubbery polymer ($P'_R(T)$ vs. $P_R(T)$) [Eq. (21)]. Again, the glass transition temperature relaxation modes (E'') are that of n-functional triglycerides as determined for hompolymerized oils (Table VI). The modulus in the rubbery region is calculated based on the crosslink density taking into account intramolecular cyclization. Therefore, the modulus for copolymers of triglycerides and styrene is [Eq. (20)]:

$$E'(T) = E_0^*[1 - P'_R(T)/100] + E'(\text{rubbery}) \qquad (20)$$

The percent of modulus loss at a given temperature in the glassy region is again the product of the mole percent triglycerides in the resin and the percent of triglycerides with T_g less than the given temperature.

The mole percent of material with effective T_g less than the temperature, $P'_R(T)$, is [Eq. (21)]:

$$P'_R(T) = P'_R(\text{glassy}) + P'_R(T_g) + P'_R(\text{rubbery}) \qquad (21)$$

Triglyceride copolymers with styrene form a single phase (one overall glass transition), but alone have very different glass transition temperatures. As a result, we expect that low crosslinked triglycerides can relax in the glassy region, but polystyrene will

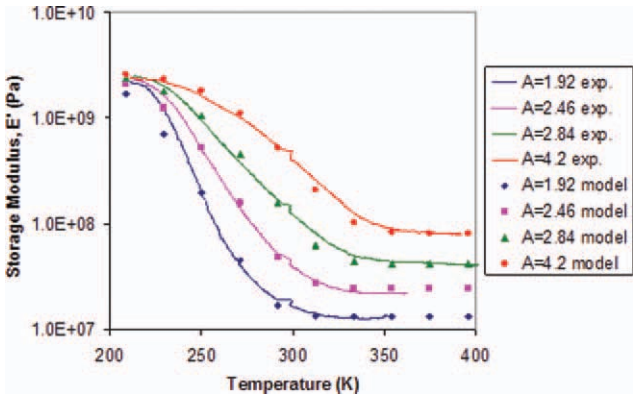

Figure 7. The storage modulus as a function of temperature as determined by experiment and as modeled for homopolymerized soybean oil acrylated to different extents. [Color figure can be viewed in the online issue, which is available at wileyonlinelibrary.com.]

not. The mole fraction of the triglycerides that relax in the glass region, P'_R(glassy) is [Eq. (22)].

$$P'_R(\text{glassy}) = \sum_{n=0}^{n} (1 - \phi_S) X_n \quad \text{for values of n where } T_g(n) < T_g^{\text{overall}} \text{ and } T_g(n) < T \quad (22)$$

where ϕ_S is the styrene mole fraction in the resin, T_g^{overall} is the overall polymer glass transition temperature based on E'', and X_n is again the mole percent of effectively polymerized n-functional triglycerides. Again, $T_g(n)$ is the glass transition temperature according to the loss modulus maximum of n-functional triglycerides.

Above the overall glass transition, high functional triglycerides with T_g above the overall polymer T_g will relax as the ambient temperature reaches the T_g of these highly functionalized/polymerized triglycerides. In addition, styrene in highly crosslinked domains that has a higher effective crosslink density than the bulk will also relax. Therefore, in the overall rubbery region, the percent of modulus loss is the percent of triglyceride and styrene connected to those triglycerides with T_g less than the given temperature [Eq. (23)].

$$P'_R(\text{rubbery}) = X_n \quad \text{for values of } n \text{ where } T_g(n) > T_g^{\text{overall}} \text{ and } T_g(n) < T \quad (23)$$

At the overall polymer glass transition, moderately functionalized triglycerides and the polystyrene within those domains will relax, even if the overall T_g is below that of polystyrene. Therefore, at the loss modulus maximum, the percent of modulus loss is the sum of the percent of triglycerides at that relaxation temperature and the remaining amount of styrene not accounted for by the other relaxation modes ($S_{\text{remaining}}$) [Eq. (24)].

$$P'_R(T_g) = X_n + S_{\text{remaining}} \quad \text{for values of } n \text{ where } T_g(n) \sim T_g^{\text{overall}} \text{ and } T_g(n) < T \quad (24)$$

This allows for the larger modulus drop in the glass transition for the styrene/triglyceride copolymers relative to the homopolymerized triglycerides. Note that whichever value of n produces a relaxation temperature closest to T_g^{overall} and is used is Eq. (24), is not used in calculation of P'_R(glassy) [Eq. (22)] and P'_R(rubbery) [Eq. (23)].

Essentially, as the temperature increases, the low functionalized triglycerides begin to soften first resulting in a modulus drop. At the overall glass transition, a larger scale blend of mid-level functional triglycerides and the styrene connected to them soften causing the modulus to drop severely. After the glass transition, high functional triglycerides and the styrene connected with those molecules soften causing the last drop in modulus before the rubbery plateau.

Figure 8 shows the storage modulus as a function of temperature for styrene/linseed oil copolymers with various levels of acrylation. The predicted modulus matched the experimentally determined modulus well as a function of temperature for various different levels of acrylation for linseed oil specifically, but also in general for any maximally acrylated oil and HOSO and soybean oil acrylated to different extents copolymerized with styrene. The model deviated for the experimental results to the largest extent when estimating the glassy region and onset of the glass transition for oils with low levels of acrylation. These slight discrepancies are likely due to slightly incorrect predictions in the triglyceride distribution and assumptions of the model [eqs. (20)–(24)].

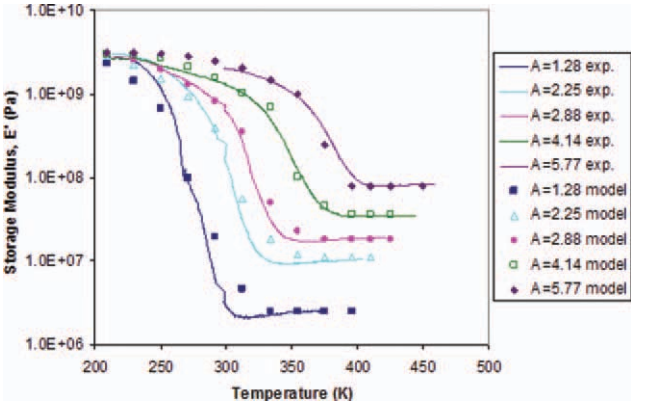

Figure 8. The storage modulus as a function of temperature as determined by experiment and as modeled for linseed oil acrylated to different extents and copolymerized with 85 mol% styrene. [Color figure can be viewed in the online issue, which is available at wileyonlinelibrary.com.]

Tan (δ) of homopolymerized triglycerides can also be predicted based on the triglyceride distribution. Given a perfect chemical network, the tan (δ) peak would be quite narrow. However, due to distributions of functionality on the crosslinkers and incomplete reaction or ineffective reaction (i.e., intramolecular cyclization), tan (δ) broadens. Viscoelasticity would indicate that the change in loss modulus relative to the storage modulus should govern tan (δ). We theorize that this change is proportional to the increase in the percentage of rubbery atoms, P_R, newly formed as the temperature is incremented from one relaxation mode/temperature to the next [Eq. (25)]:

$$\tan(\delta) \sim P_R(T_2) - P_R(T_1) \quad (25)$$

The tan (δ) curve at each relaxation temperature was modeled using the equation below for homopolymerized oils [Eq. (26)]:

$$[\tan(\delta)](T) = 0.6 \times Y(T)/(X_0 + X_1) + 0.05 \quad (26)$$

where $Y(T)$ is the percentage of the maximum functional triglycerides ($n_{\max}$) only with T_g (according to the tan (δ)) less than T [Eq. (27)]:

$$Y(T) = X_n \quad \text{for} \quad T_g(\tan(\delta), n_{\max}) < T \quad (27)$$

where T_g(tan (δ),$n_{\max}$) is the temperature corresponding to the maximum tan (δ) of the highest functional triglycerides with T_g below the temperature, T. Clearly, the T_g(tan (δ)) must be used to model the tan (δ) peak rather than $T_g(E'')$ because the maximum tan (δ) occurred at higher temperatures than the peak of

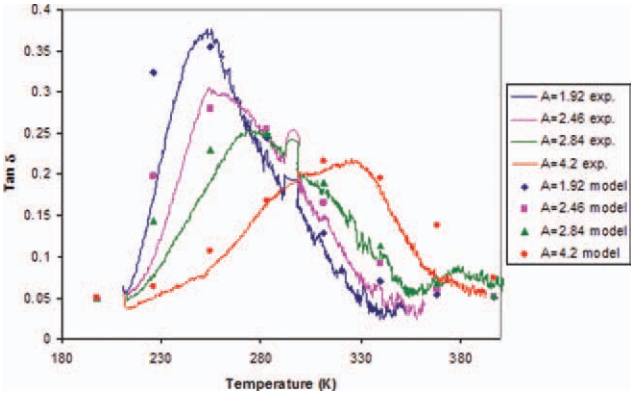

Figure 9. Experimentally measured and model prediction of the tan(δ) for homopolymerized soybean oil for different acrylation levels. [Color figure can be viewed in the online issue, which is available at wileyonlinelibrary.com.]

E''. The percentage $Y(T)$ is based on the composition of effectively crosslinked triglycerides, and is proportional to the change in rubbery content from one temperature to the other, which is in agreement with Twinkling Fractal Theory.[8] The factor of (X_0+X_1) is the percentage of uncrosslinked material (0 reacted functional groups and 1 reacted functional group, respectively) in the polymer network. This fraction is not crosslinked and therefore should act liquid-like, thus increasing tan (δ) and the loss modulus. The factor of 0.6 is a fitting parameter that accounts for the fact that the tan (δ) maximum value is modified by the percent of n-functional triglycerides and gives the predicted tan (δ) the same magnitude as the experimental results. The addition of 0.05 accounts for the fact that the value of tan (δ) is always greater than 0 for a viscoelastic material, and is also a fitting parameter. Therefore, the concept behind modeling the tan (δ) is that an n-functional triglyceride produces a tan (δ) peak at its relaxation temperature, which is a function of n. A mixture of functional triglycerides should produce a broad tan (δ) peak with a maximum at the relaxation temperature for the n-functional triglycerides with the maximum composition in the oil.

For samples copolymerized with styrene, the tan (δ) at each relaxation temperature was modeled similarly [eqs. (28)–(32)]:

$$[\tan(\delta)](T) = Y'(T)/(X_0 + X_1 + \phi_S) + 0.05 \tag{28}$$

where, similar to that of Eq. (21), $Y'(T)$ is:

$$Y'(T) = Y'(\text{glassy}) + Y'(T_g) + Y'(\text{rubbery}) \tag{29}$$

$Y'(T)$ in the glassy region is the product of the styrene mole fraction, ϕ_S, in the resin and the percent of the highest functional triglycerides with $T_g(\tan(\delta))$ below the temperature, T [Eq. (30)].

$$\begin{aligned} Y'(\text{glassy}) &= (1-\phi_S)X_n \quad \text{for} \quad T_g(\tan(\delta), n_{\max}) < T_g^{\text{overall}}(\tan(\delta)) \quad \text{and} \; T_g(\tan(\delta), n_{\max}) < T \\ &= 0 \qquad\qquad \text{for} \quad T_g(\tan(\delta), n) \geq T_g^{\text{overall}}(\tan(\delta)) \end{aligned} \tag{30}$$

Tan (δ) is thus proportional to the change in rubbery segments from one relaxation temperature to the next. At the relaxation temperatures above the glass transition temperature, $Y'(T)$ is just the percent of triglycerides at the relaxation mode with $T_g(\tan(\delta))$ less than the given temperature [Eq. (31)].

$$\begin{aligned} Y'(\text{rubbery}) &= X_n \quad \text{for} \quad T_g(\tan(\delta), n_{\max}) < T_g^{\text{overall}}(\tan(\delta)) \text{ and } T_g(\tan(\delta), n_{\max}) < T \\ &= 0 \quad \text{for} \quad T_g(\tan(\delta), n_{\max}) \leq T_g^{\text{overall}}(\tan(\delta)) \end{aligned} \tag{31}$$

At the tan (δ) maximum, $Y'(T_g)$ is the sum of the percent of triglycerides at that relaxation temperature and the remaining amount of styrene not accounted for by the relaxation modes above $T_g(\tan(\delta))$.

$$\begin{aligned} Y'(T_g) &= X_n + S_{\text{remaining}} \quad \text{for} \quad T_g(\tan(\delta), n_{\max}) < T_g^{\text{overall}}(\tan(\delta)) \text{ and } T_g(\tan(\delta), n_{\max}) < T \\ &= 0 \qquad\qquad\quad \text{for} \quad T_g(\tan(\delta), n_{\max}) < T_g^{\text{overall}}(\tan(\delta)) \\ &= 0 \qquad\qquad\quad \text{for} \quad T_g(\tan(\delta), n_{\max}) > T_g^{\text{overall}}(\tan(\delta)) \end{aligned} \tag{32}$$

This allows for a larger tan (δ) peak relative to the homopolymerized triglycerides. The uncrosslinked fraction $(X_0 + X_1 + \phi_S)$ also increases the magnitude of tan (δ) because this fraction acts liquid-like. The multiplicative coefficient in Eq. (28) (i.e., 1) is larger for the copolymerized polymers relative to the homopolymerized oils (i.e., 0.6) because the loss modulus increases as the crosslink density decreases, thus increasing tan (δ) as well. Note that whichever value of n produces a relaxation temperature closest to T_g^{overall} and is used is Eq. (32), is not used in calculation of Y'(glassy) [Eq. (30)] and Y'(rubbery) [Eq. (31)].

Figure 9 shows the tan (δ) as a function of temperature for homopolymerized soybean oil for different levels of acrylation. In general for soybean oil and other oils, the model predictions matched the experimental results. In particular, the position of the maximum was correctly modeled and the values of tan (δ) at the maximum matched the experimental results. However, the model predictions for the value of tan (δ) were slightly higher than the experimental results at temperatures approaching the tan (δ) maximum. Figure 10 shows similar correlation for tan (δ) experiment and model predictions for copolymers of

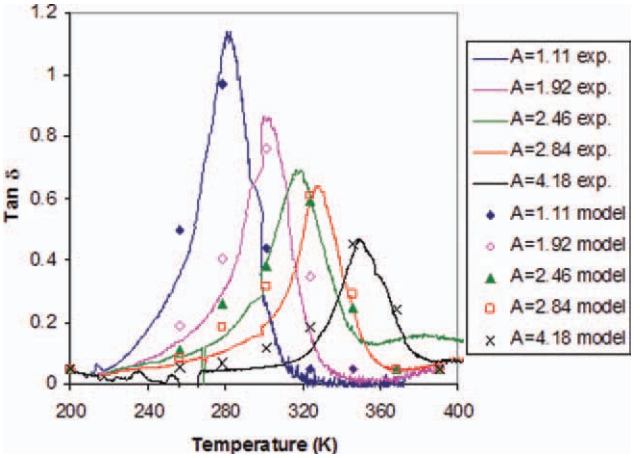

Figure 10. Experimentally measured and model prediction of the tan(δ) for copolymers of styrene and soybean oil for different acrylation levels. [Color figure can be viewed in the online issue, which is available at wileyonlinelibrary.com.]

acrylated triglycerides and styrene. Again, the model predictions for the value of tan (δ) were slightly higher than the experimental results at temperature below and above the tan (δ) maximum, but overall matched the experimental results well. Deviations between model and experiment were likely due to slightly incorrect predictions in the triglyceride distribution and the simplifying assumptions of the model [eqs. (28)–(32)].

Tan (δ) is defined as the ratio of the loss modulus and storage modulus. Thus, the loss modulus is simply the product of tan (δ) and the storage modulus [Eq. (33)]:

$$E'' = E' \times \tan(\delta) \tag{33}$$

Therefore, the loss modulus can be simply determined from the model predictions of the storage modulus and tan (δ). Figure 11 shows the predictions of the model for homopolymerized soybean oil acrylated to different extents. Figure 12 shows the

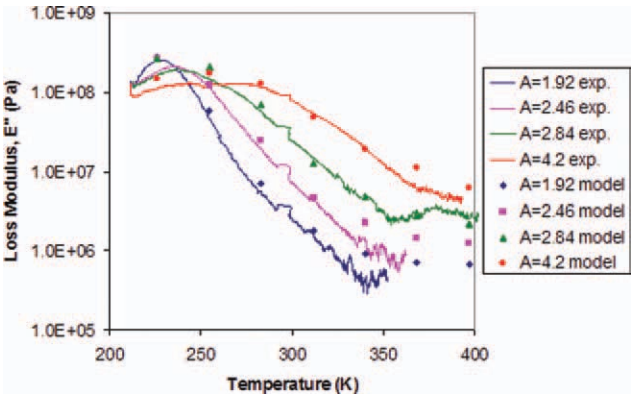

Figure 11. Experimentally measured and model prediction of the loss modulus for homopolymers of soybean oil for different acrylation levels. [Color figure can be viewed in the online issue, which is available at wileyonlinelibrary.com.]

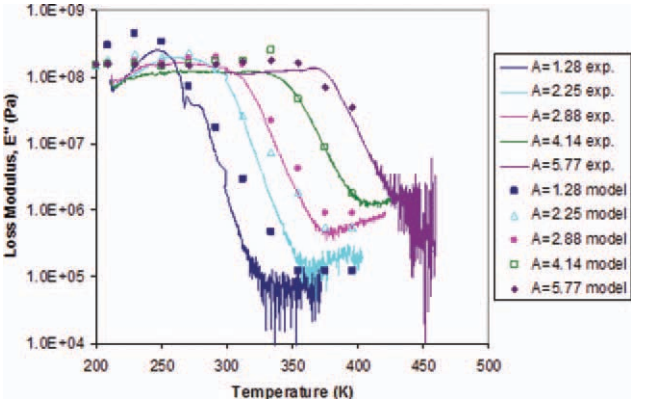

Figure 12. Experimentally measured and model prediction of the loss modulus for copolymers of styrene and linseed oil for different acrylation levels. [Color figure can be viewed in the online issue, which is available at wileyonlinelibrary.com.]

model predictions for copolymers of styrene and linseed oil for different acrylation levels. There is significant deviation between the model and experiment in the rubbery regime due to errors in prediction of tan (δ) at high temperatures. Yet overall, the model does a good job of predicting the loss modulus maximum and drop-off with temperature.

CONCLUSIONS

Triglyceride-acrylates were prepared from various plant oils and model compounds using the unsaturation sites on the triglycerides. Unlike petroleum-derived resins, acrylated plant oils have a distribution of functionality ranging from 0 through 9 acrylates per triglyceride. This distribution can be calculated using the distribution of unsaturation sites found on plant oils and then using successive binomial relationships to determine the probability of functionalizing a given functionality for a measured extent of functionalization. The crosslink densities of the resulting polymers were calculated using Flory-Stockmayer theory accounting for the extent of intramolecular cyclization.

The glass transition temperature was clearly a function of the level of acrylation of triglyceride-based polymers and was modeled using simple empirical relationships. The glass transition temperatures of *n*-acrylated triglycerides were used as the relaxation modes for plant oil-based polymers. Using these relaxation modes, the Twinkling Fractal Theory of T_g and glass transition percolation theories were extended and used in conjunction with the calculated triglyceride distribution to predict the storage modulus, tan (δ), and loss modulus as a function of temperature. Essentially, the percentage of *n*-acrylated triglycerides with T_g less than that of the ambient temperature, the rubbery fraction, is the amount the elastic modulus drops with temperature. The rubbery moduli for these polymers were calculated using the Theory of Rubber Elasticity and the calculated crosslink density. The tan (δ) was predicted based on the percentage of rubbery segments that were formed as the temperature was incremented from one relaxation mode to the next. The product of the storage modulus and tan (δ) is the loss modulus, and thus the loss modulus was also predicted based on the

polymer composition. There were some deviations between the experimental and predicted dynamic mechanical properties, but overall the model predictions matched the experimental results well. Thus, this method offers an excellent method to approximate the dynamic mechanical properties as a function of temperature for a resin containing a distribution of *n*-functional crosslinkers.

Overall, this work has three major conclusions: (1) The glass transition temperatures of *n*-functional triglycerides can be used as the relaxation temperatures for plant oil-based thermosetting polymers, (2) The calculated distribution of chemically added functionality to the triglycerides is a good estimate because of the good correspondence between model and experiment, but is also likely the main source of error between experiment and model predictions of the dynamic mechanical properties, and (3). This work provides some level of validation for the Twinkling Fractal Theory of T_g and glass transition percolation theories, as these percolation theories provide the fundamental basis of this model for predicting modulus as a function of temperature and breadth of the glass transition. Using this methodology, it may be possible to predict the thermo-mechanical properties as a function of temperature for other crosslinked systems composed of mixtures of crosslinkers with similar structure but different levels of functionality. Alternatively, this work could be used to predict the structure of the starting monomers based on the dynamic mechanical properties.

ACKNOWLEDGMENTS

This work was supported by Army Research Laboratory, the University of Delaware Army Materials Center of Excellence, NSF, EPA, and DoE for funding. The authors thank DuPont for providing the genetically engineered high oleic soybean oil and the ACRES group at the University of Delaware for helpful discussions.

REFERENCES

1. Wool, R. P.; Kusefoglu, S. H.; Palmese, G. R.; Zhao, R.; Khot, S. N. U.S. Pat. 6,121,398 (**2001**).
2. Khot, S. N.; La Scala, J. J.; Can, E.; Morye, S. S.; Williams, G. I.; Palmese, G. R.; Kusefoglu, S. H.; Wool, R. P. *J. Appl. Polym. Sci.* **2001,** *82*, 703.
3. Malik, M.; Choudhary, V.; Varma, I. K. *Rev. Macromol. Chem. Phys.* **2000,** *C40*, 139.
4. Williams, G. I.; Wool, R. P. *Appl. Comp. Matl* **2000,** *7*, 421.
5. Liu, K. Soybeans: Chemistry, Technology, and Utilization; Chapman and Hall: New York, **1997,** p 27– 30.
6. Litchfield, C. Analysis of Triglycerides; Academic Press: New York, **1972.** p 233.
7. La Scala, J. J.; Wool, R. *P. Polymer* **2005,** *46*, 61.
8. Wool, R. P. *J. Polym. Sci. Part B: Polym. Phys.* **2009,** *46*, 2765.
9. Stauffer, D.; Aharony, A. Introduction to Percolation Theory, 2nd ed.; Taylor and Francis: London, **1994,** p 147.
10. Wool, R. P. Polymer Interfaces, Structure, and Strength; Hanser Publishers: New York, **1995,** p 102.
11. La Scala, J. J.; Wool, R. P. *J. Am. Oil Chem. Soc.* **2002,** *79*, 59.
12. Gunstone, F. D. Fatty Acid and Lipid Chemistry; Blackie Academic and Professional: New York, **1996.**
13. Product Bulletin for Aerojet Accelerator, AMC-2. Rancho Cordova: Aerojet Chemicals, **2000.**
14. Fox T. G. *Bull. Am. Phys. Soc.* **1956,** *1*, 123.
15. Brill, R. P.; Palmese, G. R. *J. Appl. Polym. Sci.* **2000,** *76*, 1572.
16. Pouchert, C. J., Ed.; The Aldrich Library of Infrared Spectra, 3rd ed., Aldrich Chemical Co.: Milwaukee, **1981.**
17. Carey, F. A. Organic Chemistry, 2nd ed.; McGraw-Hill: New York, **1992,** p 529.
18. Ziaee, S.; Palmese, G. R. *J. Polym. Sci. B: Polym. Phys.* **1999,** *37*, 725.
19. Flory, P. J. Principles of Polymer Chemistry; University Press: Ithica, **1953,** p 347.
20. Nielsen, L. E.; Landel, R. F. Mechanical Properties of Polymers and Composites; Marcel Dekker: New York, **1994,** p 140.
21. La Scala, J. J.; Orlicki, J. A.; Winston, C.; Robinette, E. J.; Sands, J. M.; Palmese, G. R. *Polymer* **2005,** *46*, 2908.
22. Taheri Qazvini, N.; Mohammadi, N. *Polymer* **2005,** *46*, 9088.
23. Flory, P. J. Principles of Polymer Chemistry; University Press: Ithica, **1953,** p 432.
24. Palmese, G. R.; McCullough, R. L. *J. Appl. Polym. Sci.* **1992,** *46*, 1863.
25. Verma, D. P. S; Shoemaker, R. C. In Soybean: Genetics, Molecular Biology, and Biotechnology;Verma, D. P. S;Shoemaker, R. C., Eds.; Cab International: Wallingford, UK, **1996,** p 165.
26. Vander Wal, R. J. *J. Am. Oil Chem. Soc.* **1960,** *37*, 18.
27. Coleman, M. H.; Fulton, W. C. In Enzymes of Lipid Metabolism, Desnuelle, P., Ed.; Pergamon: Oxford, **1961,** p 127.
28. Evans, C. D.; McConnell, D. G.; List, G. R.; Scholfield, C. R. *J. Am. Oil Chem. Soc.* **1969,** *46*, 421.
29. Choi, S. C. Introductory Applied Statistics in Science; Englewood Cliffs, Prentice-Hall: NJ, **1978.**
30. La Scala, J. J.; Wool, R. P. *J. Am. Oil Chem. Soc.* **2002,** *79*, 373.
31. Flory, P. *J. J. Chem. Phys.* **1977,** *66*, 5720.
32. Painter, P. C.; Coleman, M. M. Fundamentals of Polymer Science; Technomic Publishing Company: Lancaster, PA, **1994.**
33. Ferry, J. D. Viscoelastic Properties of Polymers; Wiley: New York, **1980.**
34. Williams, M. L.; Landel, R. F.; Ferry, J. D. *J. Am. Chem. Soc.* **1955,** *77*, 3701.
35. Williams, G.; Watts, D. C. *Trans Faraday Soc.* **1970,** *66*, 80.
36. Williams, G.; Watts, D. C.; Dev, S. B.; North, A. M. *Trans Faraday Soc.* **1971,** *67*, 1323.
37. Roland, C. M.; Ngai, K. L. *Macromolecules* **1991,** *24*, 5315.
38. Pascault, J. P.; Sautereau, H.; Verdu, J.; Williams, R. J. J. Thermosetting Polymers; Marcel Dekker: New York, **2002.** p 299.
39. Nielsen, L. E. *J. Macromol. Sci. Rev. Macromol. Chem.* **1969,** *C3*, 69.